Temperature dependence of the exchange interaction and applications to electron paramagnetic resonance*

C. E. Zaspel† and J. E. Drumheller
Department of Physics, Montana State University, Bozeman, Montana 59715
(Received 21 June 1976; revised manuscript received 16 March 1977)

A previously proposed model relating the widely observed linear temperature dependence of the EPR linewidth to temperature dependence of the isotropic symmetric-exchange integral is discussed in detail and is applied to the data of several newly investigated layered structures. This model assumes an anharmonic intermolecular potential for lattice displacement and an exponential form for the exchange energy giving a temperature dependence in the paramagnetic region. Previous agreement with experimental results on $K_2CuCl_4 \cdot 2H_2O$ and some of the layered $CuCl_4$ and $MnCl_4$ compounds is now extended to include others of similar type as well as layered compounds of $CuBr_4$, $MnBr_4$, and $CuCl_2Br_2$. As before, bond strengths are taken from known tabulated results and overlap integrals are calculated with Slater-type orbitals. Arguments are presented that indicate the effect of the antisymmetric exchange cannot be the only cause for the EPR linewidth behavior.

I. INTRODUCTION

Recently attention has been given to the possibility that the exchange energy may be temperature dependent. This effect has significance since all magnetic properties are determined by the sign and magnitude of the exchange constant J. Therefore, J should be able to be determined experimentally from any cooperative magnetic effect, such as low-temperature specific heats below the transition temperature and EPR linewidth measurements in the paramagnetic region. These two methods would yield a J in different temperature regions so that if the exchange constants obtained from the two experiments are significantly different, this is an indication that J is temperature dependent. A more precise comparison between the experimental values of J in a number of layered compounds as measured by low-temperature specific heat below T_c and magnetic susceptibility above T_c has been made by deJongh,[1] however, except for $(C_2H_5NH_3)_2CuBr_4$, all cases indicated the value of J as measured above T_c to be smaller than that measured by magnetic specific heat.

Nevertheless, further support is given by Kennedy, Choh, and Seidel[2] and Okuda and Date[3] who have used the method of EPR linewidth variation and line separation as a function of temperature in $K_2CuCl_4 \cdot 2H_2O$ to measure the dependence of $J(T)$. Additional examples of temperature variation that do not seem to be caused by spin-lattice relaxation, spin-spin correlation, or antisymmetric exchange suggest that $J(T)$ may be reflected in the linewidth data in many compounds and may be due to a more basic mechanism than has been investigated before. Previously we have calculated an explicit temperature dependence of J by considering phonon modulation of the exchange integral.[4] The model associated with this calculation is very straightforward. First, the exchange integral for two bonded complexes is assumed to be an exponential function of internuclear distance. Next the thermal average of J over the vibrational states of the dimer is calculated using the vibrational states for an anharmonic oscillator.

In Sec. II below we shall look more closely at the available experimental data and in Sec. III the possible mechanisms for temperature dependence will be discussed. Section IV expands on the details of the calculation and Secs. V. and VI. will compare and discuss the temperature dependence of J predicted by this model with EPR linewidth data for several metal-organic salts.

II. EXPERIMENTAL DATA FOR $J(T)$

One of the most striking examples of a temperature-dependent exchange energy is found in $K_2CuCl_4 \cdot 2H_2O$. This compound has two separated Cu chains with inequivalent Cu sites giving g values g_1 and g_2. For exchange energies less than $J \simeq \frac{1}{2}(g_1 - g_2)\mu_B H$ there will be two resolved resonance lines.[5] If g_1 and g_2 are known, J can be estimated from the above expression for the particular magnetic field where both lines coalesce. Okuda and Date[3] used this method to obtain J for $K_2CuCl_4 \cdot 2H_2O$ between 200 and 300 °K.

At high frequencies the linewidth is[6]

$$g_{av}\mu_B \Delta H \simeq (1/8J)[(g_1 - g_2)\mu_B H]^2.$$

Kennedy, Choh, and Seidel[2] obtained J in this way between 77 and 200 °K. The temperature dependence of J for $K_2CuCl_4 \cdot 2H_2O$ from Ref. 2 is shown in Fig. 1. It can be seen that J changes by a factor

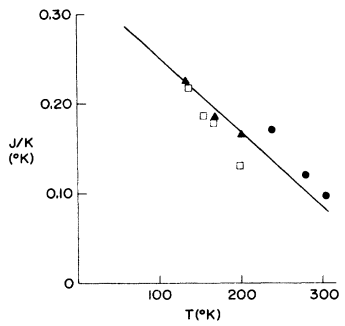

FIG. 1. Temperature dependence of the exchange interaction in $K_2CuCl_2 \cdot 2H_2O$. Circles are from the data of Okuda and Data. The triangles and squares are from EPR linewidths at 35 and 65 GHz.

of 5 between 77 °K and room temperature; also if $J(T)$ is extrapolated to low temperature, J is approximately 0.30 K which agrees very well with low-temperature specific-heat measurements.[7] Another class of compounds which appears to have a temperature dependent J are the layered structures $(C_nH_{2n+1}NH_3)_2MCl_4$, where M is either Cu^{++} or Mn^{++}, K_2CuF_4, and $Cu(HCOO)_2 \cdot 4H_2O$. These compounds have an exchange-narrowed EPR linewidth which exhibits a linear temperature dependence. For example, Yamada and Ikebe[8] found a linearly dependent linewidth for K_2CuF_4. Likewise, the layered structures $(C_nH_{2n+1}NH_3)_2CuCl_4$ also exhibit this behavior.[9] Seehra and Castner explained the linear behavior for $Cu(HCOO)_2 \cdot 4H_2O$ by phonon modulation of the antisymmetric exchange interaction.[10] For several reasons, however, the temperature dependence of the symmetric exchange J may be an equally important mechanism.

Furthermore, there are compounds that do not have an antisymmetric exchange interaction, but still have a temperature-dependent linewidth. Note, for example, the compounds $(C_nH_{2n+1}NH_3)_2MnCl_4$ mentioned above have temperature-dependent linewidths,[11] and since Mn^{++} is an S-state ion there is not normally a significant spin-orbit interaction. Recently Richards and Salamon[12] have explained the linewidth behavior for S-state antiferromagnets in the paramagnetic region, but the temperature dependence of J can also be important in these compounds. The paramagnetic dimethyl sulfoxide, $CuCl_2 \cdot 2DMSO$, also has a temperature-dependent linewidth[13] although it is not known if the dependence is linear as the measurements were only made at 77 and 300 °K. However, isotropy of the g value indicates that spin-orbit coupling is not large enough to explain the temperature dependence. Clearly at least for $K_2CuCl_4 \cdot 2H_2O$, $CuCl_2 \cdot 2DMSO$, and $(C_nH_{2n+1}NH_3)_2MnCl_4$ there must be some other mechanism responsible for the temperature-dependent linewidth.

III. DETERMINATION OF J FROM EXPERIMENTS

In this section we will discuss determination of J from EPR measurements and review the possible mechanisms resulting in a temperature-dependent linewidth; in particular, spin-spin and spin-lattice relaxation. There are two interesting cases when the spin-spin interaction is included in the Hamiltonian: the effect of exchange on the relative separation of two resolved resonance lines with different g values, and exchange narrowing of a single resonance line. The first case has been treated by Anderson[6] for two lines symmetrically spaced $\pm\omega_0$ from an arbitrary center. The exchange interaction tends to bring two lines together, and the shift from ω_0 is given by $\Delta\omega = \pm\omega_e(\omega_0^2/\omega_e^2 - 1)^{1/2}$. If ω_0 can be determined from a preferred orientation of the external field, then the exchange energy $\hbar\omega_e$ can be obtained from a measurement of $\Delta\omega$. This method was used to obtain J for the compound $K_2CuCl_4 \cdot 2H_2O$. For a single resonance line, at infinite temperature, Anderson and Weiss[5] have show that the resonance linewidth is given approximately by $\Delta\omega \propto \omega_d^2/\omega_e$, where ω_d^2 is the second moment of the resonance line, and $\omega_e = J/\hbar$. For high temperature, $kT \gg \hbar\omega_e$, strong exchange narrowing, $\omega_e \gg \omega_0$, and ignoring the temperature dependence of certain correlation functions, Richards has shown that the linewidth at finite temperature is given approximately by[14] $\Delta\omega \sim \omega_d^2/\omega_e\chi T$. Measurement of the quantity χT will now yield ω_d^2/ω_e, from which the exchange energy can be extracted if the second moment of the resonance line is known. Since χT has a negligible temperature dependence in the paramagnetic region the above expression does not adequately explain the EPR linewidth behavior. However, as noted previously, temperature dependence of the spin correlation functions in ω_d, ω_e, and χT together with an appropriate time dependence for the spin correlation functions does explain the EPR linewidth temperature dependence for antiferromagnets.

Two relaxation processes may contribute to the observed linewidth: The spin-spin relaxation with its characteristic time T_2, and the spin-lattice interaction which has a corresponding spin-lattice relaxation time T_1. If $T_1 \gg T_2$, $\Delta\omega$ is approximately $\Delta\omega \simeq 1/T_2 + 1/2T_1$ and frequently the second term can be neglected completely so J is obtained in that case from the results of Ref. 5.

By looking at the magnetic field and temperature dependence of the EPR linewidth, it should, at least in principle, be possible to determine if $\Delta\omega$

is related to T_1 or T_2. For example, if the linewidth is linear in temperature and quadratic in exernal magnetic field, then the Waller process is probably the main relaxation mechanism. If it is then determined that the temperature dependence of $\Delta\omega$ is from spin-lattice relaxation, it is then necessary to extrapolate the linewidth versus T curve to 0°K where T_1 is small. For the case when T_1 is not large, different spin-lattice relaxation mechanisms must be looked at. We will pay particular attention to these which lead to a linear dependence on field as most of the data is of this type.

First consider the Waller[15] process: a transition from state $M_s = \frac{1}{2}$ to $M_s = -\frac{1}{2}$ by interaction with a phonon of energy $g\mu_B H$. This process results in a relaxation time given by $1/T_1 \sim H^2 T$. A typical T_1 for copper is 10 sec, and a typical T_2 is 10^{-9} sec in the paramagnetic temperature region so that although this process has the appropriate linear dependence on temperature, T_1 is too long to affect the linewidth and experimentally there would be a field dependence.

Next consider a spin-phonon collision where the energy loss of a phonon is $g\mu_B H$. This is the two-phonon Raman process which was also treated by Waller. The temperature dependence of T_1 can be obtained for two cases. For low temperatures, $K_B T \ll h\omega_D$, and $1/T_1 \sim T^7$; for high temperature, $k_B T \ll h_D$, and $1/T_1 \sim T^2$. A typical Θ_D is 100 °K so $1/T_1$ usually goes as something between T^7 and T^2 for this process. In the high-temperature approximation, T_1 is still about 10 sec at 300 °K which is still much greater than T_2.

A shorter T_1 can come from modulation of the ligand field[16] which sets up an oscillating electric field as a perturbation. This perturbation will only have a direct affect on the crystal field splitting of orbital states, and the spin-phonon coupling is a second-order effect that comes from spin-orbit coupling. For the one-phonon direct process non-Kramers and Kramers ions, which have integral and half-integral spin, respectively, are investigated separately. The ground state of a non-Kramers ion can split in a crystalline field of low enough symmetry. Modulation of the Stark field then affects the spin through the spin-orbit interaction giving a temperature dependence of $1/T_1 \sim H^2 T$. At first glance it appears as if phonon modulation will not affect the ground state of a Kramers ion. However, Kronig[17] has shown that there are matrix elements due to the interaction of the Kramers state and the Stark field in the presence of an external magnetic field. For this case $1/T_1 \sim H^4 T$. At high temperature then a non-Kramers ion will have a T_1 of about 10^{-3} sec and a Kramers ion has a T_1 of 1 sec for this process, which is still long compared to T_2.

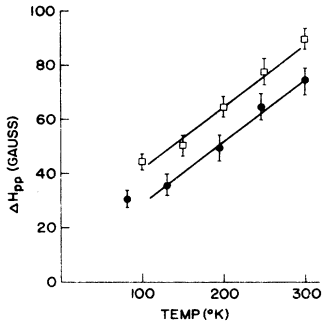

FIG. 2. EPR linewidths as a function of temperature for $(CH_3NH_3)_2CuCl_4$ at 23 and 10 GHz. The narrower lines at higher frequency could be explained by the fact the generally higher quality samples were used at the higher frequency.

In 1961, Orbach[18] was able to account for the anomalously short relaxation times by a process that is essentially an indirect transition between two Kramers states. For this process, the relaxation time is given by $1/T_1 \sim \exp(-\Delta/K_B T)$ subject to the condition $\Delta \gg k_B T$. T_1 is extremely temperature dependent since $\Delta \gg k_B T$; also T_1 can be the same order of magnitude as T_2.

There is also a two-phonon Raman process where the spin-phonon interaction comes from modulation of the ligand field. The first process arises from quadrupole transitions between the two lower non-Kramers states. The second process is similar to the two-phonon Orbach process except that it requires absorption and emission of a virtual phonon to an excited state which is outside of the phonon continuum. Both mechanisms have a temperature dependence given by $1/T_1 \sim T^7$, and a typical T_1 is 10^{-8} sec which is also comparable with T_2.

Summarizing the above it seems that no mechanisms result in a field-independent, linearly temperature-dependent linewidth, except possible the two-phonon Orbach process. Using a typical crystal field splitting for transition ions of approximately 10^3 °K it is seen that the linewidth would change by a factor of 10^4 between 100 °K and room temperature. Typical of the EPR linewidth as a function of temperature and frequency are shown in Fig. 2, in this case for $(CH_3NH_3)_2CuCl_4$. Note the linewidth is observed to change by only a factor of 2 or so in this range and is basically independent of frequency and therefore field. It would therefore appear that the relaxation processes in general including the Orbach process should be ruled out.

IV. PHONON MODULATION OF THE EXCHANGE INTEGRAL

The model previously proposed[4] involves the direct phonon modulation of the exchange integral

and was originally suggested by Harris and Owen[19] for the case of the temperature dependence of the EPR linewidths of $(NH_4)_2(Ir, Pt)Cl_6$. Also, Griffiths[20] expanded the exchange interaction in phonon operators to explain the anomalous temperature-independent spin-lattice relaxation time of diphenyl-picryl-hydrazl. More recently, Kennedy *et al.*[2] proposed that this mechanism may be responsible for the temperature-dependent exchange energy in $K_2CuCl_4 \cdot 2H_2O$. Details of the direct phonon modulation of the exchange integral for explicit temperature dependence of J are as follows.

For simplicity consider a ML_4 dimer, where M is metal and L is a ligand. If M is Cu, there is an unpaired electron in one of the metal-type molecular orbitals of the ML_4 complex. First assume that the exchange integral has the following form: $J(\delta R) = J_0 e^{-\lambda \delta R}$ for displacement δR of the distance between the two complexes. This functional form $J(\delta R)$ was used by Seehra and Castner[10] to obtain the antisymmetric exchange constant, and it was also used by Griffiths[20] because this particular form lends itself very well to expansion in terms of phonon operators.

The following method will be used to calculate $\langle J \rangle$ as a function of temperature. $\langle J \rangle$ is a thermal average over the vibrational states of the dimer, so these states are found by assuming some form for the intermolecular potential. In this model, each ML_4 complex vibrates as a single unit. Next, the matrix elements of the operator, $J(\delta R)$, are calculated for these vibrational states. Griffiths has calculated these matrix elements approximately by expanding $J(\delta R)$ in the series $J(\delta R) = J_0[1 - \lambda \delta R + \frac{1}{2}\lambda^2(\delta R)^2 = + \cdots]$ and Richards[21] considered the problem of temperature dependence by finding the thermal average of the operators $(\delta R)^2$ and $(\delta R)^3$ in the above expression. However, for typical values of the parameters, the expansion parameter $\langle \lambda \delta R \rangle$ is approximately 1, so the expansion is not justified. Therefore, it is necessary to find matrix elements of the operator $e^{-\lambda \delta R}$; then perform a thermal average over the vibrational states to obtain $\langle J \rangle$. The dimer model is then compared with the crystal by employing the Einstein approximation.

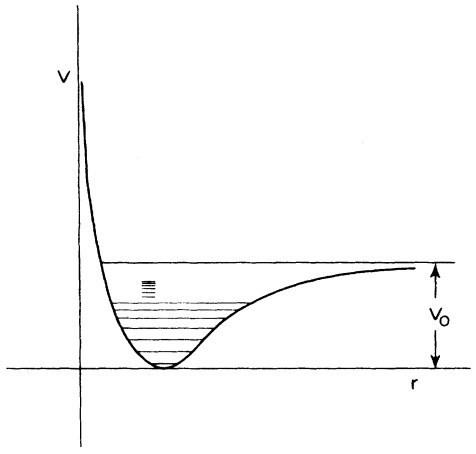

FIG. 3. Morse Potential where V_0 is the intermolecular bond strength and a is the asymmetry parameter (see text).

Any intermolecular potential can be used but a Morse function is convenient because the intermolecular potential V_0 is tabulated and also because it bears reasonable resemblence to reality. The Morse function is shown in Fig. 3 and is given by $V(r) = V_0\{1 - \exp[(r - r_0)/a]\}^2$. Here V_0 is the bond energy, r_0 is the bond length, and a is a constant that is related to the anharmonicity and frequency. Only the region where $\delta R \ll r_0$ is of interest so the potential can be expanded as $V(\delta R) \simeq V_0 + V_2 (\delta R)^2 + V_3(\delta R)^3$, where V_2 and V_3 are related to the second and third derivatives of the Morse function evaluated at the equilibrium bond length r_0.

To calculate the vibrational states, the last term in the series expansion for $V(\delta R)$ is treated as a perturbation, $H' = V_3(\delta R)^3$. The unperturbed state is just the harmonic oscillator wave function, and addition of the perturbation results in the anharmonic oscillator problem. The matrix elements $I_n = (n|J(\delta R)|n)$ to second order are evaluated and are listed in the Appendix. The matrix element I_n contains matrix elements connecting states differing by more than 6. However, to be consistent with second-order perturbation results, matrix elements of the form $\langle m|J|n\rangle$ for $|n - m| > 6$ are dropped.

With each of these terms evaluated, the thermal average of $\langle J(\delta R) \rangle$ is $\langle J(\delta R) \rangle = \sum_n P_n I_n$, where P_n is the probability of the system being in the nth vibrational state;

$$P_n = \sum_s \frac{e^{-E_n^0/kT}}{e^{-E_s^0/kT}}$$

It is possible to eliminate the anharmonicity parameter a by comparing the Morse function with the exchange energy. Since the bond energy is indeed closely related to the exchange energy, it is reasonable to assume that both have the same exponential form. This implies that $a \simeq 1/\lambda$, so now it is only necessary to obtain λ, V_0, and the reduced mass of the oscillator. Here it is convenient to define the dimensionless parameter $Y = \lambda\hbar/2(2mV_0)^{1/2}$ or, using the second derivative of the Morse potential, $Y = \lambda^2\hbar/2m\omega$. Y can also be expressed in terms of frequency. Note, Y is the argument of the Laguerre polynomials that result

TABLE I. Values of λ for divalent-metal–monovalent-halides bonds. All numbers are to be multiplied by 10^8 cm^{-1}.

	F^-	Cl^-	Br^-	I^-	At^-
Sc^{++}	3.26	2.76	2.50	2.38	2.31
Ti^{++}	3.47	2.97	2.71	2.58	2.52
V^{++}	3.67	3.17	2.90	2.78	2.72
Cr^{++}	3.91	3.38	3.11	2.99	2.92
Mn^{++}	4.09	3.58	3.32	3.20	3.13
Fe^{++}	4.28	3.78	3.52	3.40	3.33
Co^{++}	4.49	3.99	3.73	3.60	3.54
Ni^{++}	4.70	4.20	3.94	3.81	3.75
Cu^{++}	4.90	4.40	4.13	4.01	3.94

from the matrix element integration.

Next a value of λ is calculated for the appropriate metal-ligand ($M-L$) bond. This will be done by comparing the exponential part of a $M-L$ overlap integral

$$S = \int \psi_m(X)\psi_L(X+R)\,dx$$

with $e^{-\lambda\delta R}$. We are only interested in the radial part of S, so Slater-type orbitals will be used for ψ_M and ψ_L. The Slater-type orbital for an atomic orbital is[22]

$$\psi = Nr^{n^*-1}e^{-(Z^*/n^*)r},$$

where r is measured from the nucleus of the atom in atomic units, N is a normalization constant, n^* is an effective quantum number, and Z^* is the effective nuclear charge defined by $Z^* = Z - s$, where s is the screening constant. Both n^* and s are calculated from the rules given by Slater,[22] which are reproduced here for convenience:

(1) For $n = 1,2,3,4,5,6$; n^* is given the following values:

$n^* = 1,2,3,3.7,4.0,4.2$.

(2) Electrons are divided into the groups indicated in parentheses:

$(1s),(2s,2p),(3s,3p)(3d),(4s,4p)(4d),(4f),$ $(5s,5p)$, etc.

For any group of electrons, s has the following contributions:

(a) Zero for any electron outside the group;

(b) an amount of 0.35 for each other electron in the group unless the group is 1s, then 0.30 is used;

(c) an amount of 0.85 for each electron in a shell with total quantum number less by 1 and 1.0 for each electron further in; if the group is d or f, an amount of 1.0 for every electron further in.

For the case of Cu(II), which has the configuration $(1s^2)(2s^22p^6)(3s^23p^6)3d^9$, the shielding constant for each group inside the d group is $2(1.0)+8(1.0)+8(1.0)+8(.35)=20.8$ and the corresponding Z^* is 5.2. This procedure may be used for the other transition metals and the halides.

Using these orbitals, S can be integrated, but this is not necessary since only the exponential part of $\exp\frac{1}{2}(-Z_m^*/n_m^*-Z_L^*/n_L^*)$ is needed. Z^*/n^* is given in units of inverse Bohr radii. Z^* and n^* are used in the above expression to obtain S for different $M-L$ bonds which immediately yields a value for the overlap parameter λ which are indicated in Table I.

The bond energy V_0 is not known for most of the compounds of interest. However, the bond energy can be estimated from the postulate of the geometric mean, which was proposed by Pauling.[23] For a heteronuclear diatomic molecule, this postulate relates the bond energy in kcal/mole to the homonuclear bond energy of each atom by the relation: $D(M-L)=[D(M-M)D(L-L)]^{1/2}+30(x_M-x_L)^2$. $D(M-L)$ and $D(L-L)$ are the bond energies of the metal and ligand homonuclear diatomic molecules, and the last term accounts for the extra bond energy resulting from partial ionic character of the bond if there is a difference in electronegativity x_M and x_L of the metal and the ligand. The homonuclear bond strength and electronegativity can be obtained from standard references[24]; these quantities, as well as $D(M-L)$, are listed in Table II.

The next step is to relate the calculated or measured bond energy to the bond energy of the compounds. This is done by comparing the metal-ligand bond length of the particular compound to a calculated bond length corresponding to the above energy. For example, if the bond length corresponding to the geometric mean bond energy is less than the metal-ligand bond length of the compound, then the postulate of the geometric mean gives an estimate of the bond energy that is probably too high, and a suitable correction will have to be made.

To be consistent, the bond lengths are calculated from an equation containing the covalent radii and the electronegativity difference[23]:

$$R(M-L) = r_M + r_L - 0.06\,|x_M - x_L| \qquad (1)$$

TABLE II. Homonuclear bond strengths, electronegativity, and bond strengths for metals and ligands.

Bond	$D(M-M)$ (kcal/mole)	$D(L-L)$ (kcal/mole)	x_M	x_L	$D(M-L)$ (kcal/mole)
Cu-F	47.0	37.7	1.9	4.0	78.5
Cu-Cl	47.0	57.9	1.9	3.0	89.0
Cu-Br	47.0	46.3	1.9	2.8	71.3
Mn-Cl	22	57.9	1.5	3.0	70.0
Mn-Br	22	46.3	1.5	2.8	70.0

TABLE III. Covalent radii and bond distances for metal-legand bonds.

Bond	r_M	r_L	$\lvert x_M - x_L \rvert$	$R(M\text{-}L)$	R(measured)
Cu-Cl	1.35	0.99	1.1	2.27	2.79 $(NH_4)_2CuCl_4$
					2.79 $(CH_3NH_3)_2CuCl_2Br_2$
					2.79 $(C_3H_7NH_3)_2CuCl_2Br_2$
					2.92 $(C_6H_5NH_3)_2CuCl_4$
Cu-F	1.35	0.63	2.1	1.85	2.08 K_2CuF_4
Cu-Br	1.35	1.11	0.9	2.41	(2.94) $(C_3H_7NH_3)_2CuBr_4$
Mn-Cl	1.18	0.99	1.5	2.08	2.63 $(C_3H_7NH_3)_2MnCl_4$
Mn-Br	1.18	1.11	1.3	2.21	(2.78) $(C_3H_7NH_3)_2MnBr_4$

in units of Å. $R(M\text{-}L)$ is indicated in Table III for different metal-ligand bonds, and they are compared with some of the measured bond lengths of different compounds. Apparently the calculated bond lengths are too short, which means that the calculated bond energy is too large, and it has to be adjusted to agree with the longer bonds. This is done with an equation proposed by Pauling[23]:

$$R(n) = R(M\text{-}L) - 0.60 \log_{10} n \tag{2}$$

Here n is the bond number and we assume that the bond strengths are related to the calculated bond strengths by

$$V(n) = nV(M\text{-}L). \tag{3}$$

$R(n)$ and $R(M\text{-}L)$ are the bond lengths for the corresponding bond numbers. Now if $V(M\text{-}L)$ and $R(M\text{-}L)$ are known, the bond strength $V(n)$ can be calculated from Eqs. (2) and (3) and $V(n)$ is the bond strength for the particular measured bond length. This bond energy $V(n)$ is used along with λ and the reduced mass m of the particular oscillator to arrive at the parameter Y. The bond numbers and bond strengths for several compounds are shown in Table IV. Tables III and IV also contain the data for layered structures of $CuBr_4$,[25] and $MnBr_4$.[26]

V. THEORETICAL RESULTS

As an example, an estimate of Y is now made for $K_2CuCl_4 \cdot 2H_2O$. This compound can be thought of as an aggregate of K ions, $CuCl_2 \cdot H_2O$ molecules, and Cl ions. The oscillator we will consider is two weakly bonded $CuCl_2 \cdot 2H_2O$ molecules which has a reduced mass of 1.4×10^{-22} g; λ obtained from Table I for the Cu-Cl bond is 4.4×10^8 cm^{-1}; and V_0 from Table IV is 0.61×10^{-12} erg. These numbers correspond to a Y of about 0.02, which in turn results in a vibrational frequency of 6.8×10^{12} Hz. Since $\hbar\omega \simeq kT$ at room temperature the thermal average is over the first 20 vibrational states as a resonable approximation. The family of curves for $\langle J \rangle$ versus temperature for the weakly bonded $CuCl_4$ complex was given previously but the similar curves for the CuF_4 complexes is illustrated in Fig. 4. In each family the oscillator reduced mass is a constant, and V_0 are variables in the parameter Y. For small Y, roughly between 0.01 and 0.005, $\langle J \rangle$ has little temperature dependence; however, the exchange integral becomes very temperature dependent as Y is increased to 0.04 or 0.05. The experimental results of Kennedy *et al.*, shown in Fig. 1, agree very well with the $\langle J \rangle$ curve for $Y = 0.02$ for the $CuCl_4$ model. One would also expect compounds with a temperature

TABLE IV. Bond numbers and bond strenghts for metal-legand bonds.

Bond	n	$V(1)$ (ergs)	$V(n)$ (ergs)
Cu-Cl	0.10	6.12×10^{-12}	0.612×10^{-12} $K_2CuCl_4 \cdot 2H_20$
	0.083	6.12	0.51 $(C_6H_5NH_3)_2CuCl_4$
Cu-Cl	0.18	6.12	1.10 $(NH_4)_2CuCl_4$
	0.18	6.12	1.10 $(C_3H_7NH_3)_2CuCl_2Br_2$
			1.10 $(CH_3NH_3)_2CuCl_2Br_2$
Cu-F	0.61	4.90	2.98 K_2CuF_4
Cu-Br	0.15	5.49	0.82 $(C_3H_7NH_3)_2CuBr_4$
Mn-Cl	0.13	4.80	0.63 $(C_3H_7NH_3)_2MnCl_4$
Mn-Br	0.11	5.22	1.41 $(C_3H_7NH_3)_2MnBr_4$

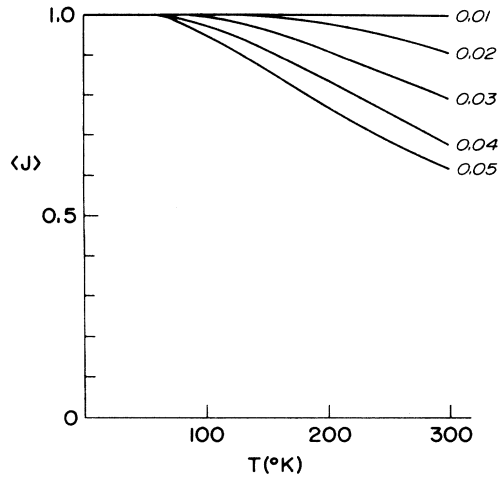

FIG. 4. Exchange energy J vs temperature for CuF_4. Solid lines are for $Y = \lambda h/2(2mV_0)^{1/2}$ where λ is related to the overlap integral and V_0 is the bond energy for the dimer. All curves are normalized to one at 0 °K.

dependent J to exhibit a relatively large thermal expansion. $K_2CuCl_4 \cdot 2H_2O$, for example, has a thermal expansion of 10^{-4} K^{-1}, which implies a 3% change in the lattice constant between 0 °K and room temperature. The exponential $e^{-\lambda\delta R}$ then changes by roughly a factor of 2. This shows good correspondence with the $Y = 0.02$ curve for $CuCl_4$.

A suitable model for the manganese compounds may also be developed. For $(CH_3NH_3)_2$ $MnCl_4$ all the planar Mn-Cl bonds are equal and relatively long compared to the out of plane Mn-Cl bonds; so each plane is composed of Cl ions and $MnCl_2$ complexes. $\langle J(T)\rangle$ is then calculated for the $MnCl_2$-Cl-$MnCl_2$ molecule, and the results are shown in Fig. 5. It is also interesting to note that $\langle J\rangle$ becomes extremely temperature dependent in

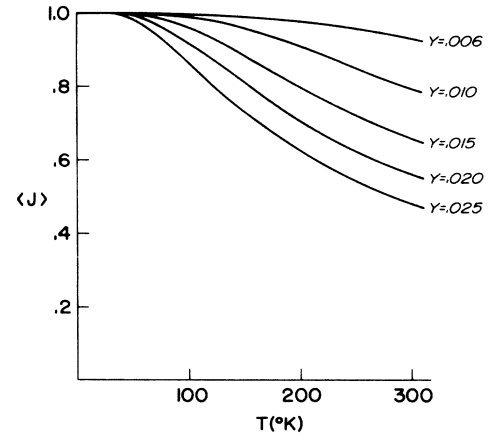

FIG. 5. Exchange energy vs temperature for the $MnCl_2$-Cl-$MnCl_2$ molecule. Solid lines are for $Y = \lambda h/2(2mV_0)^{1/2}$. All curves are normalized to 1 at 0 °K.

only a relatively small range of Y but for most values of Y has little temperature dependence. This seems to explain why strongly bonded transition-metal salts such as MnF_2 and $CuF_2 \cdot 2H_2O$ show little or no indication of a temperature-dependent exchange energy while the more weakly bonded $(CH_3NH_3)_2$ $MnCl_4$ shows significant dependence. The case of $CrBr_3$ has also been studied[27] but is rather unique because of the unknown nature of the bonds so it is not included here.

VI. RESULTS AND DISCUSSION

For both K_2CuF_4 and $(C_nH_{2n+1}NH_3)_2CuCl_4$ the phonon structures are similar with weakly bonded $CuCl_4$ complexes so the CuF_4 and $CuCl_4$ dimers will be the oscillators in the calculation of $\langle J\rangle$. From Tables I and II the values for overlap parameters and bond strengths for K_2CuF_4 are 5.4×10^8 cm^{-1}, and 2.6×10^{-12} erg which corresponds of a Y of 0.02 using the CuF_2 dimer. Similarly, the appropriate bond strength and overlap parameter from the tables yield $Y = 0.02$ for the layered compounds $(C_nH_{2n+1}NH_3)_2$ $CuCl_4$. Figure 6 indicates that J has little temperature dependence of K_2CuF_4,[28] therefore, the temperature-dependence linewidth is probably the result of antisymmetric exchange. The $1/J$ versus temperature curve for the $CuCl_4$ dimer agrees very well with experimental linewidth measurements on n-polypylammonium tetrachlorocuprate $(C_2N_7NH_3)_2CuCl$ indicated on Fig. 6.

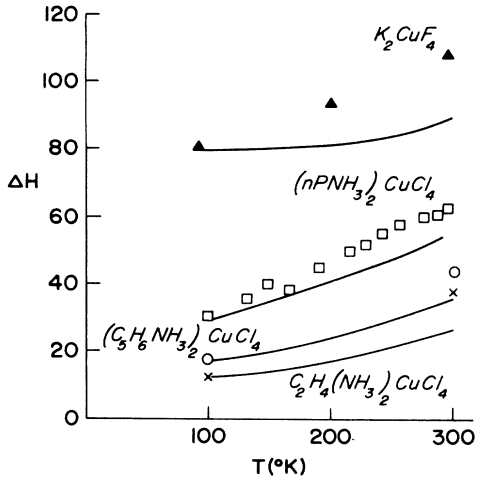

FIG. 6. EPR linewidth vs temperature for K_2CuF_4 and several layered $CuCl_4$ compounds. The triangles are for K_2CuF_4 and the squares, circles, and crosses are for $(nP\text{-}NH_3)_2CuCl_4$, $(C_5H_6NH_3)_2CuCl_4$, $C_2H_4(NH_3)_2CuCl_4$, respectively, and the solid lines are the calculated linewidths for the appropriate values of the parameter Y. The theoretical curves are normalized so that the calculated and experimental linewidths are the same at 100 °K, and the units on the vertical axis are gauss.

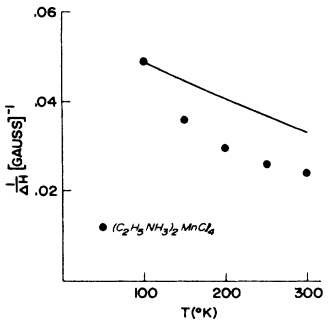

FIG. 7. Inverse EPR linewidth vs temperature for $(C_2H_5NH_3)_2MnCl_4$. The circles are experimental points, and the solid line is for $Y=0.015$ from Fig. 6.

Also shown in Fig. 6 are the results for $(C_6H_5NH_3)_2CuCl_4$ and $[C_2H_4(NH_3)_2]CuCl_4$. Castner and Seehra have shown that if one considers phonon modulation of the antisymmetric exchange term, the linewidth is linearly related to temperature, $\Delta H \sim J^4(\Delta g/g)^2 T$. For K_2CuF_4, [29] $J/k = 11.2\,^{\circ}K$ and $\Delta g/g = 0.21$; similarly $(CH_3NH_3)_2\,CuCl_4$ has a J/k and $\Delta g/g$ given by $12.2\,^{\circ}K$ and 0.07, respectively. Apparently, the slope of the linewidth versus temperature curve for K_2CuCl_4 should be roughly a factor of 10 greater than for the layered compound; however, since this is not observed experimentally we attribute the temperature dependence in the $(C_nH_{2n+1}NH_3)_2\,CuCl_4$ and related layer series to a direct modulation of the isotropic exchange energy. Finally, an appropriate Y for $(C_2H_5NH_3)_2MnCl_4$ is 0.015. The temperature dependence of J is compared with the linewidth data for this compound in Fig. 7. Here the phonon modulation of the exchange integral at least partially explains the temperature EPR linewidth; the remaining temperature dependence can probably be explained by Richard's theory.

APPENDIX

The harmonic oscillator states are calculated with

$$H' = V_3(\delta R)^3$$

as a perturbation. In terms of creation and destruction operators,

$$R = i(\hbar/2m\omega)^{1/2}(a^\dagger - a)$$

the perturbation is

$$H' = -iV_3\left(\frac{\hbar}{2m\omega}\right)^{3/2}(a^\dagger a^\dagger a^\dagger - a^\dagger a a^\dagger - a^\dagger a^\dagger a + a^\dagger a a - a a^\dagger a^\dagger + a a a^\dagger + a a^\dagger a - a a a).$$

Starting with the zeroth-order state $|n\rangle$, the first- and second-order corrections to $|n\rangle$ are now calculated. The first-order correction is

$$|\psi_n'\rangle = -iV_3\left(\frac{\hbar}{2m\omega}\right)^{3/2}\frac{[(n+1)(n+2)(n+3)]^{1/2}}{E_n^0 - E_{n+3}^0}|n+3\rangle - \frac{(n+1)^{3/2}}{E_n^0 - E_{n+1}^0}|n+1\rangle - \frac{n(n+1)^{1/2}}{E_n^0 - E_{n+1}^0}|n+1\rangle + \frac{(n-1)\sqrt{n}}{E_n^0 - E_{n-1}^0}|n-1\rangle$$
$$- \frac{(n+2)(n+1)^{1/2}}{E_n^0 - E_{n+1}^0}|n+1\rangle + \frac{(n+1)\sqrt{n}}{E_n^0 - E_{n-1}^0}|n-1\rangle + \frac{n^{3/2}}{E_n^0 - E_{n-1}^0}|n-1\rangle - \frac{[n(n-1)(n-2)]^{1/2}}{E_n^0 - E_{n-3}^0}|n-3\rangle,$$

and the second-order correction is

$$|\psi_n^2\rangle = -\left(\frac{\hbar}{2m\omega}\right)^3 V_3^2\left(\frac{[(n+1)\cdots(n+6)]^{1/2}}{(E_n^0 - E_{n+6}^0)(E_n^0 - E_{n+3}^0)}|n+6\rangle - \frac{(n+2)^{3/2}(n+1)^{3/2}}{(E_n^0 - E_{n+2}^0)(E_n^0 - E_{n+1}^0)}|n+2\rangle\right.$$
$$- \frac{n(n+1)[(n+1)(n+2)]^{1/2}}{(E_n^0 - E_{n+2}^0)(E_n^0 - E_{n+1}^0)}|n+2\rangle + \frac{(n-1)(n-2)[n(n-1)]^{1/2}}{(E_n^0 - E_{n-2}^0)(E_n^0 - E_{n-1}^0)}|n-2\rangle$$
$$- \frac{(n+2)(n+3)[(n+1)(n+2)]^{1/2}}{(E_n^0 - E_{n+2}^0)(E_n^0 - E_{n+1}^0)}|n+2\rangle + \frac{n(n+1)[n(n-1)]^{1/2}}{(E_n^0 - E_{n-2}^0)(E_n^0 - E_{n-1}^0)}|n-2\rangle$$
$$\left. + \frac{(n-1)^{3/2}n^{3/2}}{(E_n^0 - E_{n-2}^0)(E_n^0 - E_{n-1}^0)}|n-2\rangle - \frac{[n\cdots(n-5)]^{1/2}}{(E_n^0 - E_{n-6}^0)(E_n^0 - E_{n-3}^0)}|n-6\rangle\right),$$

Where ω is defined by $\hbar\omega = E_{n+1}^0 - E_n^0$.

The anharmonic oscillator state is now

$$|n\rangle = |n\rangle + |\psi_n^1\rangle + |\psi_n^2\rangle.$$

Now the matrix element I_n is calculated:

$$I_n = \langle n|J(\delta R)|n\rangle + \langle\psi_n^1|J(\delta R)|\psi_n^1\rangle + \langle\psi_n^2|J(\delta R)|\psi_n^2\rangle + 2\langle n|J(\delta R)|\psi_n^1\rangle + 2\langle n|J(\delta R)|\psi_n^2\rangle + 2\langle\psi_n^1|J(\delta R)|\psi_n^2\rangle.$$

Since I_n must be real, the following terms are zero:

$$\langle n|J(\delta R)|\psi_n^1\rangle, \langle\psi_n^1|J(\delta R)|\psi_n^2\rangle.$$

Each of the other four expressions are evaluated separately in terms of harmonic oscillator states $|n\rangle$. $\langle n|J(\delta R)|n\rangle$ is already in the desired form; the other two are

$$\langle n|J(\delta R)|\psi_n^2\rangle = \left(\frac{\hbar}{2m\omega}\right)^3 V_3^2 \left(- \frac{[(n+1)\cdots(n+6)]^{1/2}}{(E_n^0 - E_{n+6}^0)(E_n^0 - E_{n+3}^0)} \langle n|J(\delta R)|n+6\rangle \right.$$
$$+ \frac{[(n+1)(n+2)]^{1/2}[2(n+1)^2 + (n+2)(n+3)]}{(E_n^0 - E_{n+2}^0)(E_n^0 - E_{n+1}^0)} \langle n|J(\delta R)|n+2\rangle$$
$$- \frac{[n(n-1)]^{1/2}[(n-1)(n-2) + 2n^2]}{(E_n^0 - E_{n-2}^0)(E_n^0 - E_{n-1}^0)} \langle n|J(\delta R)|n-2\rangle$$
$$\left. + \frac{[(n-5)\cdots n]^{1/2}}{(E_n^0 - E_{n-6}^0)(E_n^0 - E_{n-3}^0)} \langle n|J(\delta R)|n-6\rangle \right),$$

$$\langle \psi_n^1|J(\delta R)|\psi_n^1\rangle = \left(\frac{\hbar}{2m\omega}\right)^3 V_3^2 \left(\frac{(n+1)(n+2)(n+3)}{(E_n^0 - E_{n+3}^0)^2} \langle n+3|J(\delta R)|n+3\rangle \right.$$
$$+ \frac{[(n+1)^{3/2} + n(n+1)^{1/2} + (n+2)(n+1)^{1/2}]^2}{(E_n^0 - E_{n+1}^0)^2} \langle n+1|J(\delta R)|n+1\rangle$$
$$+ \frac{[n^{3/2} + (n+1)n^{1/2} + (n-1)n^{1/2}]^2}{(E_n^0 - E_{n-1}^0)^2} \langle n-1|J(\delta R)|n-1\rangle$$
$$+ \frac{n(n-1)(n-2)}{(E_n^0 - E_{n-3}^0)^2} \langle n-3|J(\delta R)|n-3\rangle$$
$$- 2\frac{(n+1)^{3/2}[(n+1)(n+2)(n+3)]^{1/2}}{(E_n^0 - E_{n+3}^0)(E_n^0 - E_{n+1}^0)} \langle n+1|J(\delta R)|n+3\rangle$$
$$+ 2\frac{[(n+1)(n+2)(n+3)]^{1/2}[n^{3/2} + n^{1/2}(n+1+n^{1/2}(n-1)]}{(E_n^0 - E_{n+3}^0)(E_n^0 - E_{n-1}^0)} \langle n-1|J(\delta R)|n+3\rangle$$
$$- 2\frac{[(n-2)(n-1)\cdots(n+3)]^{1/2}}{(E_n^0 - E_{n+3}^0)(E_n^0 - E_{n-3}^0)} \langle n-3|J(\delta R)|n+3\rangle$$
$$- 2\frac{(3n+3)(n+1)^{1/2} + 3n\sqrt{n}}{(E_n^0 - E_{n+1}^0)(E_n^0 - E_{n-1}^0)} \langle n-1|J(\delta R)|n+1\rangle$$
$$+ 2\frac{(3n+3)[(n+1)n\cdots(n-2)]^{1/2}}{(E_n^0 - E_{n+1}^0)(E_n^0 - E_{n-3}^0)} \langle n+1|J(\delta R)|n-3\rangle$$
$$\left. - 2\frac{3n^2[(n-1)(n-2)]^{1/2}}{(E_n^0 - E_{n-1}^0)(E_n^0 - E_{n-3}^0)} \langle n-1|J(\delta R)|n-3\rangle \right).$$

Next it is necessary to evaluate matrix elements of the form

$$\langle k|J(\delta R)|l\rangle,$$

which is equivalent to the following integral:

$$I_{nn} = \frac{J_0}{2^n n!} \frac{1}{\sqrt{\pi}} \int_{-\infty}^{\infty} \exp\left(-\nu^2 - \frac{\lambda}{a}\nu\right) H_n(\nu)\, d\nu$$

for the diagonal matrix element here $a = (m\omega/\hbar)^{1/2}$. This can be evaluated:

$$I_{nn} = J_0 e^{\lambda^2/4a^2} L_n^0(-\lambda^2/2a^2),$$

and the off-diagonal matrix elements are

$$I_{kl} = \frac{J_0}{2^{(k+l)/2}(k!\,l!)^{1/2}} e^{\lambda^2/4a^2} 2^l k! \left(-\frac{\lambda}{2a}\right)^{l-k} \times L_l^{l-k}\left(-\frac{\lambda^2}{2a^2}\right)$$

for $l > k$. L_l^{l-k} is an associated Laguerre polynomial with a negative argument. The necessary matrix elements are

$$\langle n|\, J(\delta R)|\, n\rangle = J_0 e^{Y/2} L_n^0(-Y),$$

$$\langle n+1|\, J(\delta R)|\, n+3\rangle = 2J_0 Y e^{Y/2} \frac{L_{n+3}^2(-Y)}{[(n+2)(n+3)]^{1/2}},$$

$$\langle n-1|\, J(\delta R)|\, n+3\rangle = 4J_0 Y^2 e^{Y/2} \frac{1}{[n\cdots(n+3)]^{1/2}} \times L_{n+3}^4(-Y),$$

$$\langle n-3|\, J(\delta R)|\, n+3\rangle = 8J_0 Y^3 e^{Y/2} \frac{1}{[(n-2)\cdots(n+3)]^{1/2}} \times L_{n+3}^6(-Y),$$

$$\langle n-1|\, J(\delta R)|\, n+1\rangle = 2J_0 Y e^{Y/2} \frac{1}{[n(n+1)]^{1/2}} L_{n+1}^2(-Y),$$

$$\langle n-3|\, J(\delta R)\,|\, n+1\rangle = 4J_0Y^2e^{Y/2}\,\frac{1}{[(n-2)\cdots(n+1)]^{1/2}} \times L^4_{n+1}(-Y),$$

$$\langle n-3|\, J(\delta R)\,|\, n-1\rangle = 2J_0Ye^{Y/2}\,\frac{1}{[(n-2)(n-1)]^{1/2}} \times L^2_{n-1}(-Y),$$

$$\langle n|\, J(\delta R)\,|\, n+6\rangle = 8J_0Y^3e^{Y/2}\,\frac{1}{[(n+1)\cdots(n+6)]^{1/2}} \times L^6_{n+6}(-Y),$$

$$\langle n|\, J(\delta R)\,|\, n+2\rangle = 2J_0Ye^{Y/2}\,\frac{1}{[(n+1)(n+2)]^{1/2}} \times L^2_{n+2}(-Y),$$

$$\langle n|\, J(\delta R)\,|\, n-2\rangle = 2J_0Ye^{Y/2}\,\frac{1}{[n(n-1)]^{1/2}} \times L^2_{n}(-Y),$$

$$\langle n|\, J(\delta R)\,|\, n-6\rangle = 8J_0Y^3e^{Y/2}\,\frac{1}{[(n-5)\cdots n]^{1/2}} \times L^6_{n}(-Y).$$

These integrals are now used in each term of the expression for I_n with the parameter Y used as the variable.

$$\begin{aligned}\langle \psi^1_n|\, J(\delta R)\,|\, \psi^1_n\rangle =& J_0\tfrac{1}{4}Ye^{Y/2}[\tfrac{1}{9}(n+1)(n+2)(n+3)L^0_{n+3}(-Y)\\ &+9(n+1)^3L^0_{n+1}(-Y)+9n^3L^0_{n-1}(-Y)+\tfrac{1}{9}n(n-1)(n-2)L^0_{n-3}(-Y)]\\ &+J_0\tfrac{1}{2}Ye^{Y/2}[-(n+1)^2YL^2_{n+3}(-Y)-nY^2L^4_{n+3}(-Y)\\ &+\tfrac{1}{9}Y^3L^6_{n+3}(-Y)+3(2n+1)YL^2_{n+1}(-Y)-(n+1)Y^2L^4_{n+1}(-Y)-nYL^2_{n-1}(-Y)],\end{aligned}$$

$$\begin{aligned}\langle n|\, J(\delta R)\,|\, \psi^2_n\rangle =& J_0\tfrac{1}{16}Ye^{Y/2}\{-\tfrac{1}{18}Y^3L^6_{n+6}(-Y)+\tfrac{1}{2}[2(n+1)^2+(n+2)(n+3)]YL^2_{n+2}(-Y)\\ &+\tfrac{1}{2}[2n^2+(n-2)(n-1)]YL^2_n(-Y)+\tfrac{1}{18}Y^3L^6_n(-Y)\}.\end{aligned}$$

*Partial support for this work is given by the NSF.

†Present address: Physik Institut der Universität Zürich, Zürich, Switzerland.

[1]L. J. DeJongh and A. R. Miedema, Adv. Phys. 23, 1 (1974).
[2]T. A. Kennedy, S. H. Choh, and G. Seidel, Phys. Rev. B 2, 3645 (1970).
[3]T. Okuda and M. Date, J. Phys. Soc. Jpn. 28, 308 (1970).
[4]C. E. Zaspel and J. E. Drumheller, Solid State Commun. 17, 1107 (1975).
[5]P. W. Anderson and P. R. Weiss, Rev. Mod. Phys. 25, 269 (1953).
[6]P. W. Anderson, J. Phys. Soc. Jpn. 9, 316 (1954).
[7]A. R. Miedema, R. F. Wielinga, and W. J. Huiskamp, Physica (Utr.) 31, 1585 (1965).
[8]I. Yamada and M. Ibeke, J. Phys. Soc. Jpn. 33, 1334 (1972).
[9]J. E. Drumheller, D. H. Dickey, R. P. Reklis, C. E. Zaspel, and S. J. Glass, Phys. Rev. B 5, 4631 (1972).
[10]M. S. Seehra and T. G. Castner, Phys. Kondens. Mater. 7, 185 (1968).
[11]H. R. Boesch, U. Schmocker, F. Waldner, K. Emerson, and J. E. Drumheller, Phys. Lett. A 36, 461 (1971).
[12]P. M. Richards and M. B. Salamon, Phys. Rev. B 9, 32 (1974).
[13]T. Reddy and R. Srinivasan, J. Chem. Phys. 45, 2714 (1966).
[14]P. M. Richards, Phys. Rev. 142, 189 (1966).
[15]I. Waller, Z. Phys. 79, 370 (1932).
[16]J. Van Vleck, Phys. Rev. 57, 426 (1940).
[17]R. Kronig, Physica (Utr.) 6, 33 (1939).
[18]R. Orbach, Proc. R. Soc. Lond. A 264, 458 (1961).
[19]A. Harris and J. Owen, Proc. R. Soc. Lond. A 289, 122 (1966).
[20]R. B. Griffiths, Phys. Rev. 124, 1023 (1961).
[21]P. M. Richards (private communication).
[22]J. Slater, Phys. Rev. 42, 33 (1932).
[23]L. Pauling, *The Nature of the Chemical Bond* (Cornell U.P., Ithaca, N.Y., 1960).
[24]*Handbook of Chemistry and Physics*, 47th ed., edited by R. C. Weast (The Chemical Rubber Company, Cleveland, Ohio, 1966).
[25]R. E. Willett and M. Extine, Chem. Phys. Lett. 23, 281 (1973).
[26]R. D. Willett and M. Extine, Phys. Lett. A 44, 503 (1973).
[27]J. E. Drumheller and C. L. Zaspel, Proceedings of the International Conference on Magnetism, Amsterdam, 1976 (to be published).
[28]We had previously reported (see Ref. 2) a higher temperature dependence for K_2CuF_2 based on a Cu-F-Cu model. We also had earlier assumed the K_2CuF_2 structure to be centro-symmetric which is not the case: see Ref. 29 below and D. I. Khomskii and K. I. Kugel, Solid State Commun. 13, 763 (1973).
[29]L. Khoi and P. Veillet, Phys. Rev. B 11, 4128 (1975).